Talanta 253 (2023) 124021

Contents lists available at ScienceDirect

Talanta

journal homepage: www.elsevier.com/locate/talanta

A new multi-factor multi-objective strategy based on a factorial presence-absence design to determine polymer additive residues by means of head space-solid phase microextraction-gas chromatography-mass spectrometry

Lucía Valverde-Som [a], Ana Herrero [a], Celia Reguera [a], Luis Antonio Sarabia [b], María Cruz Ortiz [a,*]

[a] Department of Chemistry, Faculty of Sciences, Universidad de Burgos, Plaza Misael Bañuelos s/n, 09001, Burgos, Spain
[b] Department of Mathematics and Computation, Faculty of Sciences, Universidad de Burgos, Plaza Misael Bañuelos s/n, 09001, Burgos, Spain

ARTICLE INFO

Keywords:
D-optimal design
HS-SPME-GC-MS
PARAFAC2
Multi-objective optimization
Plastic additive residues
Natural mineral water

ABSTRACT

A new multi-factor multi-objective strategy to approach the joint assessment of the effect of six experimental factors in the determination by head space-solid phase microextraction-gas chromatography-mass spectrometry (HS-SPME-GC-MS) of eight different additives commonly used in the plastic packaging manufacturing is proposed in this work. Five HS-SPME experimental factors, both qualitative and quantitative, are explored: the type of fiber, addition of salt, extraction and desorption time, and extraction temperature. The effect of these factors is studied through a factorial presence-absence model, that include interactions, using a D-optimal design. As a result, the number of experiments is reduced from 128, full factorial design, to 14. The effect of carrying out the measurements in different experimental sessions is considered by including a blocking factor. The response for each compound is estimated in the experimental domain and then the best experimental conditions are chosen by using Pareto front. Parallel coordinates are employed to show the conflicting conditions intrinsic to a multi-objective analysis when compounds of different nature are extracted by HS-SPME. Parallel factor analysis 2 (PARAFAC2) decomposition is used because it makes the determination of target compounds in the presence of unknown interferents possible, which enables the unequivocal identification of target compounds according to official regulations. The developed method is applied to determine 2,6-di-tert-butyl-4-methyl-phenol (BHT), benzophenone (BP), bis(2-ethylhexyl) adipate (DEHA), diethyl phthalate (DEP), diisobutyl phthalate (DiBP), dibutyl phthalate (DBP), benzyl butyl phthalate (BBP) and bis(2-ethylhexyl) phthalate (DEHP). The level of these compounds found in nine types of bottled natural still and sparkling mineral waters is very low, so the compounds were not present in quantities that may be injurious to human health.

1. Introduction

Solid phase microextraction (SPME) is a sample preparation technique of such a nature as to allow extract and concentrate analytes in the sample. It does not require long extraction times and large amounts of solvents to maximize recovery, as the most of extraction techniques commonly used to isolate target analytes, in fact, it is relatively fast and uses no extraction solvent. Likewise, SPME can handle small sample volumes (whether solid, liquid or gaseous samples) and is easily automated for high-throughput analysis, e.g. coupled to GC-MS or LC-MS [1]. Reviews of SPME can be found in literature [2,3], where recent applications and advances of the extraction technique are reviewed and discussed.

However, a limitation of the SPME method is that each application requires its own separate method development procedure since the extraction conditions have to be suitable for all of the target analytes in the sample matrix. There are many parameters (such as mode of extraction, fiber coating or extraction and desorption conditions) that have to be set and optimized during SPME method development depending on the sample matrix and on the properties of the target analytes [4,5]. In addition, sample modifications, including salt addition or pH adjustment, are usually performed to improve transfer of the target analytes from the sample to the headspace when the headspace (HS) extraction mode is used.

* Corresponding author.
E-mail address: mcortiz@ubu.es (M.C. Ortiz).

https://doi.org/10.1016/j.talanta.2022.124021
Received 16 May 2022; Received in revised form 11 October 2022; Accepted 13 October 2022
Available online 17 October 2022

Therefore, to study a large number of experimental variables when developing a SPME method is necessary [5]. The conventional 'one--variable-at-a-time' approach [6], where the variables are analysed by changing one factor at a time, keeping other variables constant, do not address interactions among variables, which are expected to be significant [7]. So, multifactorial statistical approaches such as design-of-experiments methodology is particularly helpful [8,9].

Nowadays, identification of the main dependent factors which are supposed to affect the most the analysis, considering a limited number of levels of those experimental factors, is increasingly often a common approach in the development of novel SPME methods [10–12], in HS-SPME-GC-MS too. Recently, a Box-Behnken design is used by Biancolillo et al. [13] to optimize sample temperature, sample conditioning time and extraction time in the study of organosulfur volatile profiles of Italian red garlic, or by Muñoz-Redondo et al. [14] to optimize extraction temperature, extraction time, ionic strength and dilution of the sample for the analysis of terpenoids in sparkling wines. A central composite design is used by Pico et al. [15] to optimize three experimental factors (sample quantity, extraction temperature and extraction time) in the determination of volatile compounds in blueberries by SPME-GC-MS. On the other hand, Vieira et al. [16] use a definitive screening designs, a three-level screening design, to analyse eight factors (degas, sample volume, addition of salt, type of fiber, agitation, pre-incubation time, extraction time and extraction temperature) in the analysis of key flavour compounds in wort and beer by HS-SPME-GC-MS.

The more factors and factor levels are considered in the optimization study, the greater the number of experiments required in the experimental designs. D-optimal designs [17], based on the D-optimality concept, have proved to be a very suitable tool for approaching this issue because they are chosen when the classical designs cannot be used, such as when the number of experiments is too large [7,18–20].

In addition, as previously stated, the selected conditions have to be suitable for all the target analytes since they may be present simultaneously in a sample; therefore, a multi-target analysis has to be considered [21]. However, optimal conditions are often not common and conflict with each other; the greater the number of analytes are, the more likely the conditions are to be contradictory. Different methods have been proposed to perform the optimization of multiple responses with the aim of choosing a good enough alternative from several possibilities. Examples of the use of Derringer's desirability function [22] for multi-target optimization in SPME can be found in literature [14,15,23], as well as of the Pareto optimal front approach [17,24,25].

To quantify the analytes, a multi-way technique has also been used. PARAFAC (parallel factor analysis) [26] or PARAFAC2 [27,28] methods, which have the second-order advantage, makes it possible to determine target compounds in the presence of non-calibrated interferents. Both methods have proved very useful for solving the interference of non-target compounds and/or unexpected interferents [29], in the optimization of SPME procedures too [23,30], deriving a powerful tool from their combination with D-optimal designs [7,31,32]. PARAFAC2 is the structural model appropriate for handling shifts in the chromatographic mode, as justified in Annex.

Multivariate curve resolution coupled to alternating least squares, MCR-ALS, is an alternative when, because of a serious trilinearity failure, the PARAFAC or PARAFAC2 structural models are not suitable to describe the experimental data tensor [33,34]. As in all bilinear models, MCR-ALS has rotational ambiguity, i.e. the solution obtained is not unique and then there is no guaranty that it matches with the chromatographic and/or spectral profiles of the analytes. Methods to assess this ambiguity have been newly developed [35,36]. In addition, in each particular case, if the knowledge about the structure of the data is used and appropriate constraints are imposed, it is possible to reduce that ambiguity [37].

A methodology that combine D-optimal design, multi-objective analysis and PARAFAC2 was developed in this work to assess the relative effect of six experimental factors on nine responses in the determination of eight polymer additive residues (and the internal standard) in bottle natural still and sparkling mineral waters by HS-SPME-GC-MS. Applications of HS-SPME for the analysis of water samples can be found in literature [38,39]; some of them dedicated to the determination of some plastic additives (plasticizers, stabilizers …) in bottled water, which may come from migration during storage or the manufacturing process itself [40], together to other non-intentionally added substances [41].

The developed procedure was applied to determine eight different additives commonly used in the packaging manufacturing: 2,6-di-tert-butyl-4-methyl-phenol (BHT), used as an antioxidant; benzophenone (BP), which is a UV stabilizer that protect the polymer from UV light-induced degradation; and an adipate, bis(2-ethylhexyl) adipate (DEHA), and five phthalates, diethyl phthalate (DEP), diisobutyl phthalate (DiBP), dibutyl phthalate (DBP), benzyl butyl phthalate (BBP) and bis(2-ethylhexyl) phthalate (DEHP), which are plasticizers. These compounds may present a risk to public health, as in the case of some phthalates which have been demonstrated to be endocrine disruptors.

2. Material and methods

2.1. Chemicals

Benzophenone (BP, CAS no. 119-61-9, purified by sublimation, ≥ 99% purity), benzyl butyl phthalate (BBP, CAS no. 85-68-7, analytical standard, ≥ 98% purity), bis(2-ethylhexyl) adipate (DEHA, CAS no. 103-23-1, ≥99% purity), bis(2-ethylhexyl) phthalate (DEHP, CAS no. 117-81-7, analytical standard, ≥ 98% purity), 2,6-di-tert-butyl-4-methyl-phenol (BHT, CAS no. 128-37-0, ≥99% purity), dibutyl phthalate (DBP, CAS no. 84-74-2, analytical standard, ≥ 98% purity), diethyl phthalate (DEP, CAS no. 84-66-2, 99.5% purity), diisobutyl phthalate (DiBP, CAS no. 84-69-5, 99% purity), and diisobutyl phthalate-3,4,5,6-d_4 (DiBP-d_4, CAS no. 358730-88-8, ≥98% purity), used as internal standard (IS), were purchased from Sigma-Aldrich (Steinheim, Germany). Granular sodium chloride (CAS no. 7647-14-5), in glass container, was purchased from Avantor Performance Materials (Center Valley, PA). Acetone (CAS no. 67-64-1), methanol (CAS no. 67-56-1) and n-hexane (CAS no. 110-54-3), for liquid chromatography Lichrosolv® were from Merck KGaA (Darmstadt, Germany). A Milli-Q gradient A10 water purification system from Millipore (Bedford, MA, USA) was used to obtain Milli-Q water.

Helium (99.999% purity, ALPHAGAZ™ 1, Air Liquide, Madrid, Spain) was used as the carrier gas.

2.2. Standard solutions

Stock solutions of BHT at 2700 mg L^{-1}, of DEP, DiBP, DEHA at 2000 mg L^{-1}, of BP at 1000 mg L^{-1}, DBP and DEHP at 700 mg L^{-1} and of DiBP-d_4 and BBP at 500 mg L^{-1} were prepared individually in methanol. All intermediate standard solutions were prepared in methanol. The final solutions were prepared from 50 μL of the last intermediate solution by dilution to 10 mL with Milli-Q water or saturated sodium chloride Milli-Q water. These final solutions were put into 20 mL glass vials for SPME.

All the stock and intermediate solutions were under gravimetric control, to verify that the solvent has not evaporated, and stored in crimp vials, protected from light, at 4 °C. All intermediate and final solutions were prepared daily.

2.3. Bottled water samples

Seven bottled natural mineral still waters and two carbonated waters of different commercial brands were purchased at local stores (Burgos, Spain). There were analysed still and sparkling waters bottled in different containers: i) glass, ii) transparent polyethylene terephthalate (PET), iii) colour PET, and iv) recycled PET (RPET), with different

percentages of recycled plastic (25%, 50% and 100%). Table 1 shows the description of the nine studied samples; three bottles of each sample (Di_j) were analysed.

Prior to analysis, carbonated water samples were placed in an ultrasound bath and left for 60 min. Every sample was saturated with sodium chloride and then 10 mL of the saturated solution with 2 μg L^{-1} of IS was placed into a 20 mL glass vial for SPME.

2.4. Instrumentation

All chromatographic separations were performed using an Agilent 6890N gas chromatograph with a split-splitless injector, coupled to an Agilent 5975 mass spectrometer detector with a single quadrupole mass analyser (Agilent Technologies, Palo Alto, CA, USA). A glass liner for SPME (0.75 mm ID) was used. The analytical column was a capillary column with dimensions of 30 m × 0.25 mm inner diameter × 0.25 μm film thickness and coated with a (5%-phenyl)-methylpolysiloxane stationary phase (Agilent HP-5MS Ultra Inert column, J&W Scientific, Folsom, CA, USA). The SPME procedure was performed using a TriPlus autosampler equipped with a SPME module (Thermo Scientific, Milan, Italy). Two fibers were used for the SPME: polydimethylsiloxane/divinylbenzene (PDMS/DVB, 65 μm film thickness, fiber 1) and divinylbenzene/carboxen on polydimethylsiloxane (DVB/CAR/PDMS, 50/30 μm film thickness, fiber 2); both were supplied by Supelco (Bellefonte, PA, USA).

2.5. HS-SPME-GC-MS experimental procedure

Before the first use, both fibers were conditioned according to the specifications of the manufacturer (fiber 1: 250 °C for 30 min; fiber 2: 270 °C for 30 min). Different methods were created according to a D-optimal experimental design. The incubation time was maintained at 2 min in all experiments. The extraction temperature and the extraction and desorption time were changed based on the corresponding experimental plan. Both incubation and extraction steps were carried out with constant stirring. The injection port temperature for fiber 1 was 250 °C, and 270 °C for the second one; the depth of penetration of the needle in the injector was 27 mm. Helium was used as the carrier gas at a flow rate of 1.3 mL min^{-1} and the initial pressure was set at 69.8 kPa.

The oven temperature was 40 °C for a certain time after injection (2 or 5 min according to the experimental plan), as a function of desorption time and then was increased at 20 °C min^{-1} to 250 °C, which was held for 1 min. That temperature was ramped again at 10 °C min^{-1} to 280 °C, which was held for 1 min. The run time was 20.50 min for 5 min desorption time and 17.50 min for 3 min. In all experiments, a post-run step was carried out at 300 °C for 3 min.

After each extraction/desorption process, fibers were cleaned-up at their corresponding conditioning temperature for 6 min. At the beginning and at the end of each chromatographic sequence, system blanks (vials with no solution) were injected to control the clean-up of the whole HS-SPME-GC-MS system.

The mass spectrometer operated in the electron impact (EI) ionization mode at 70 eV. The transfer line temperature was set at 300 °C, the ion source at 230 °C and the quadrupole at 150 °C. After a solvent delay of 9.4 min or 12.4 min, according to the desorption time, the data were acquired in single ion monitoring mode using the eight acquisition windows which are shown in Table 2. When desorption time was set at 2 min, 3 min must be subtracted from the start time of each acquisition window since the injection time was shortened by up to 3 min.

Bottled water samples were saturated with sodium chloride and analysed using a DVB/CAR/PDMS fiber, extraction temperature of 80 °C, extraction time of 40 min and desorption time of 5 min (conditions obtained from the experimental design).

The laboratory glassware used throughout the work was thoroughly cleaned twice with three solvents (n-hexane, acetone and methanol, in this order) and plastic consumables were avoided as far as possible.

2.6. Samples and data arrays

The GC-MS data recorded in the different steps of the study were arranged in several data arrays, for each chromatographic window after baseline correction, in a three-way array X of dimension (I × J × K); the

Table 1
Information regarding the bottled natural mineral water samples and packaging.

Sample code	Packaging					Waters
	Material	Volume (mL)	Colour	Recycled (%)	Cap colour	
D1_1	RPET	750	Blue	100	White	Still
D1_2	RPET	500	Uncoloured	100	Red	Still
D1_3	PET	2000	Uncoloured	–	Red	Still
D2_1	RPET	1500	Blue	50	White	Still
D2_2	RPET	500	Uncoloured	50	Blue	Still
D2_3	RPET	500	Uncoloured	25	Grey	Still
D3_1	PET	330	Uncoloured	–	Red	Still
D3_2	Plastic*	500	Green	–	Green	Sparkling
D3_3	Glass	250	Uncoloured	–	Grey metal	Sparkling

RPET: recycled polyethylene terephthalate; PET: polyethylene terephthalate; (*) not indicated.

Table 2
Distribution of segments used for the selective monitoring of each analyte for desorption time 5 min (3 min must be subtracted from the start time of each window when desorption time 2 min is considered).

Window	Start time (min)	Ion dwell time (ms)	Analyte	*m/z* ratios
BHT	12.40	30	BHT	91, 145, 177, 205[a], 220
DEP	13.10	30	DEP	105, 121, 132, 149[a], 177
BP	13.45	30	BP	51, 77, 105[a], 152, 182
DiBPs	14.20	10	IS	80, 153[a], 171, 209, 227
			DiBP	104, 149[a], 167, 205, 223
DBP	15.10	30	DBP	104, 121, 149[a], 205, 223
BBP	16.40	30	BBP	91, 104, 149[a], 206, 238
DEHA	17.65	30	DEHA	112, 129[a], 147, 241, 259
DEHP	18.40	30	DEHP	71, 149[a], 167, 207, 279

([a]) Base peak.

Table 3
Dimension of data arrays (scans × ions × samples) and characteristics of PARAFAC2 models (number of factors, explained variance and CORCONDIA index) built for each acquisition window in the different steps of this work.

Step of the study		Model	BHT	DEP	BP	DiBP and IS	DBP	BBP	DEHA	DEHP
Experimental design	Day 1	Array dimension	30 × 5 × 7	63 × 5 × 7	70 × 5 × 7	95 × 10 × 7	79 × 5 × 7	53 × 5 × 7	40 × 5 × 7	74 × 5 × 7
		# Factors	1	1	2	3	2	1	1	2
		Expl. Var (%)	99.94	99.95	99.94	99.99	99.99	99.78	99.90	99.98
		CORCONDIA (%)	100	100	100	99	100	100	100	100
	Day 2	Array dimension	30 × 5 × 7	63 × 5 × 7	70 × 5 × 7	95 × 10 × 7	79 × 5 × 7	53 × 5 × 7	40 × 5 × 7	74 × 5 × 7
		# Factors	1	1	2	3	2	1	1	2
		Expl. Var (%)	99.94	99.95	99.98	100	100	99.78	99.96	99.97
		CORCONDIA (%)	100	100	99	100	100	100	100	100
Tolerance intervals		Array dimension	30 × 5 × 5	63 × 5 × 5	70 × 5 × 5	95 × 10 × 5	79 × 5 × 5	53 × 5 × 5	40 × 5 × 5	74 × 5 × 5
		# Factors	2	1	1	2	1	1	1	1
		Expl. Var (%)	100	99.96	99.60	99.99	99.99	99.84	99.98	99.97
		CORCONDIA (%)	100	100	100	100	100	100	100	100
Linear dynamic range		Array dimension	30 × 5 × 16	63 × 5 × 16	70 × 5 × 16	95 × 10 × 16	79 × 5 × 16	53 × 5 × 16	40 × 5 × 16	74 × 5 × 16
		# Factors	2	1	1	3	1	1	1	1
		Expl. Var (%)	99.98	99.95	99.60	100	99.99	99.84	99.98	99.97
		CORCONDIA (%)	100	100	100	100	100	100	100	100
Bottled water analysis	Day 1	Array dimension	30 × 5 × 33	63 × 5 × 33	70 × 5 × 33	95 × 10 × 33	79 × 5 × 33	53 × 5 × 33	40 × 5 × 33	74 × 5 × 33
		# Factors	2	1	2	3	2	1	1	2
		Expl. Var (%)	99.94	99.95	99.96	100	100	99.77	99.91	99.97
		CORCONDIA (%)	100	100	100	100	100	100	100	100
	Day 2	Array dimension	30 × 5 × 33	63 × 5 × 33	70 × 5 × 33	95 × 10 × 33	79 × 5 × 33	53 × 5 × 33	40 × 5 × 33	74 × 5 × 33
		# Factors	2	1	1	3	2	1	1	2
		Expl. Var (%)	99.78	99.95	99.95	100	100	99.75	99.92	99.94
		CORCONDIA (%)	100	100	100	100	100	100	100	100
	Day 3	Array dimension	30 × 5 × 33	63 × 5 × 33	70 × 5 × 33	95 × 10 × 33	79 × 5 × 33	53 × 5 × 33	40 × 5 × 33	74 × 5 × 33
		# Factors	2	1	1	2	2	1	1	2
		Expl. Var (%)	99.97	99.95	99.59	99.99	100	99.77	99.96	99.96
		CORCONDIA (%)	100	100	100	100	100	100	100	100

first way being the chromatographic way (I elution times), the second one the spectral way (J diagnostic ions), and the third one the sample way (K samples). The dimension of the data arrays is shown in Table 3.

The experimental design step involved a standard solution which was analysed over 2 days by applying 14 different HS-SPME procedures of an experimental plan. To determine the tolerance intervals, 5 reference standards were prepared: three of them at 3 different concentration levels of the target analytes (covering the wider range of concentrations used) and a fixed level of IS, and the other 2 at different concentrations of IS and a fixed level of the target analytes. The linear dynamic range was estimated from 16 injections: 2 system blanks, 12 standards with increasing concentrations of the target analytes and a fixed level of IS, and the remaining 2 standards where only the concentration of IS changed.

In the last step of the study, standards, fortified blank samples and bottled water samples were analysed over 3 days in such a way that a total of 33 injections were done each day: 2 system blanks, 12 standards with increasing concentrations of the target analytes and constant concentration of IS, 2 standards with fixed concentrations of the target analytes and different levels of IS, 8 fortified blank samples (only 5 the 3rd day) and 9 bottled water samples (12 samples the 3rd day). The data arrays corresponding to these analyses were used to determine detection capability of the analytical procedure, the precision and the concentration of the target analytes in the bottled water samples.

2.7. Software

Scan control and data acquisition were performed using an MSD ChemStation version D.02.00.275 (Agilent Technologies, Inc.) with Data Analysis software. The TriPlus autosampler was controlled by means of TriPlus Sampler version 1.6.9 SPME (Thermo). PLS_Toolbox software, version 9.0 Eigenvector Research Inc. (Wenatchee, WA, USA, 2021), for use within the MATLAB environment, version 9.10.0.1739362 (R2021a, Mathworks, Inc., Natick, MA, USA, 2021), was used to perform the PARAFAC2 decompositions. The program COO-FRO [42] was used to obtain the coordinates parallel plot and Pareto front. STATGRAPHICS Centurion XVIII, version 18.1.11 (Statpoint Technologies, Inc., Herndon, VA, USA, 2018) was used to fit and validate the regression models. DETARCHI program [43] was used to calculate the critical value (x_C) and minimum detectable value (x_D) of the concentration. The D-optimal designs were built with NEMRODW, version 2015 (L.P.R.A.I., Marseille, France, 2015).

3. Results and discussion

3.1. Analysis of the HS-SPME experimental factors

As mentioned above, many parameters are involved in SPME. Considering all of these factors [5], the type of fiber, addition of salt to the aqueous medium, extraction and desorption time, and extraction temperature have been considered in this work. The levels of these factors and those of other experimental parameters were chosen based on literature and on preliminary results.

Thus, two fibers based on DVB and on a combination of DVB and Carboxen® (CAR) both embedded in polymeric films of polydimethylsiloxane (PDMS) were chosen. PDMS/DVB fibers have been widely used in the determination of plastic additives in different matrices [44–46] as well as DVB/CAR/PDMS fibers [47–49], where the combination of DVB and CAR makes them particularly interesting to cover an extended molecular weight range, although they have slightly lower capacity for lighter or heavier analytes in comparison to the single sorbent fibers.

The levels for extraction temperature were set at 70 and 80 °C, usual values found for these kind of compounds [44,47]; high enough to promote their evaporation but to avoid water boiling which may damage the fiber. Extraction time is a crucial parameter because it also influences the partition equilibria. A wide range of values can be found in literature of up to 60 min [45,47,48], but such long times are not generally needed. In order to not excessively extend the total analysis time of each sample, four levels of extraction times were studied in this work, from 10 to 40 min, in 10 min increments. Desorption times of 2 and 5 min were chosen [47,48].

On the other hand, the presence of salt in the aqueous medium can promote the mass transfer of target analytes to the headspace [44, 47–49], mainly for compounds with log P < 3, although it could negatively affect those most polar. For that reason, the addition of salt has been considered as a factor with two levels, adding salt or not [45].

In addition to the five factors referred to above, a block factor is included in the design so that in the event that the experimental design cannot be completed in a single laboratory session the day-to-day variability is considered. Therefore, based on the analysis of the literature made above, the six factors in Table 4 were considered in the design, all of them at two levels except for extraction time that was at four levels.

3.1.1. Construction of the D-optimal experimental design

The experimental design methodology is the appropriate tool for exploring the effect of the six factors at the levels in Table 4 on the yield of the HS-SPME and then to decide the conditions in which the best results are achieved. The use of this methodology requires defining the experimental domain and the functional model that relate factors and levels with the experimental response. In this case, the experimental domain is constituted by the 128 combinations of the factors at the levels in Table 4.

Only when a linear model (in the coefficients) is proposed to relate factors and responses, and it is estimated by least squares, it is possible to factorize the variability in coefficients and responses in two factors: 1) the variability due to the arrangement of the experiments in the domain, and 2) the experimental variability. In this way, the experiments to be performed can be selected in such a way that the quality of estimate is not undermined. Additionally, it is possible to check the compatibility of the chosen model with the experimental data. Such a strategy is not possible when other types of regression are used as a neural network.

The functional model for factors with a different number of levels, as that in Table 4, is the "presence-absence" model. This model requires to define a "reference level" and is used in such a way that the effect of changing the factor to another level is evaluated in relation to the reference level. In this case, the reference level is L2 for factors 1 to 5 and L4 for the sixth. As a consequence, a binary variable is required for factors 1 to 5 and three variables for factor 6 (Table 4). The variables x_{iA}, i = 1, …,5, are 1 when the i-th factor is at level A and −1 when is at level B. To indicate that factor 6 is at level A, variables x_{6A}, x_{6B} and x_{6C} are 1, 0, and 0, respectively; and these variables take the values 0, 1 and 0 when it is at level B, 0, 0 and 1 for level C, and finally, −1, −1 and −1 for level D. Therefore, the model, with one order interactions to relate the experimental response, y, to factor and level indicator variables, x_{ij}, is given by equation (1); with 34 coefficients, b, that, except b_0, are the value of the effect of each factor and interaction on the response.

$$y = b_0 + \sum_{i=1}^{5} b_{iA}x_{iA} + \sum_{k=A}^{C} b_{6k}x_{6k} + \sum_{i=1}^{5}\sum_{j>i}^{5} b_{iAjA}x_{iA}x_{jA} + \sum_{i=1}^{5}\sum_{k=A}^{C} b_{iA6k}x_{iA}x_{6k} \quad (1)$$

At least 34 experiments are thus necessary to estimate this model, which still requires a great experimental effort. However, it is not expected that most of these interactions will have effect on the response, such as interaction 1–4 (block - to add salt). If the interaction between factors 5 and 6 (extraction temperature and extraction time) is considered as the only interaction that could have effect, the model is reduced to that in equation (2), which have 12 coefficients.

$$y = b_0 + \sum_{i=1}^{5} b_{iA}x_{iA} + \sum_{k=A}^{C} b_{6k}x_{6k} + \sum_{k=A}^{C} b_{5A6k}x_{5A}x_{6k} \quad (2)$$

This means that at least 12 experiments, chosen among those of the full factorial design which are 128 ($2^5 \times 4$) for levels and factors in Table 4, are required to estimate this model. A D-optimal design [17], which provides an "ad-hoc" experimental design for the problem at hand, was used to decide what experiments, among the 128, should be carried out. This is a well-established procedure to reduce the experimental effort to that strictly necessary in order to precisely estimate the main effects and the interactions of interest that have been established a priori by using the model in equation (2).

To define the D-optimal design, the starting point is a search space, in this case the 128 possible experiments of the full factorial design. For each size, $n > 12$, the set of n experiments that provide the joint estimate of the 12 coefficients with the best possibly precision was searched; this is the D-optimal design for that value of n and may be not unique. Then, the maximum variance inflation factor (VIF) for each coefficient was examined; it has to be the smaller as possible. For $n = 14$ there are two D-optimal designs, 1.39 being the lowest maximum for the VIF. For this design, the VIF for the estimate of each coefficient in equation (2), other than b_0, ranges from 1.19 to 1.39. This is therefore a design very appropriate to precisely estimate the effect of the factors and interaction through the coefficients of model in equation (2). Table 5 shows the experiments of the D-optimal design chosen which was used to carry out the study.

Table 4
Level coding and variable name, in the model, for the factors of the SPME optimization.

	Factor	Level/code				Variable		
		L1/A	L2/B	L3/C	L4/D			
1	Block (day)	1	2	–	–	x_{1A}		
2	Type of fiber	1	2	–	–	x_{2A}		
3	Desorption time (min)	2	5	–	–	x_{3A}		
4	To add salt	no	yes	–	–	x_{4A}		
5	Extraction temperature (°C)	70	80	–	–	x_{5A}		
6	Extraction time (min)	10	20	30	40	x_{6A}	x_{6B}	x_{6C}

3.1.2. Experimentation and obtention of the responses

The experiments in Table 5 were conducted by applying the experimental procedure in section 2.5 to samples containing 0.4 μg L^{-1} of BHT, 10 μg L^{-1} of DEP, 2 μg L^{-1} of BP and IS, 1 μg L^{-1} of DiBP, 4 μg L^{-1} of DBP, 200 μg L^{-1} of BBP, 100 μg L^{-1} of DEHA and 300 μg L^{-1} of DEHP. Fig. 1(a–b) shows the chromatograms recorded from the HS-SPME conditions of experiments 37 and 24 in Table 5, respectively. It is clear that the size of the different chromatographic peaks depends very much on the experimental conditions set at the HS-SPME step under study.

On completion of the 14 experiments, for each chromatographic window, the GC-MS data obtained were arranged in a three-way array as explained in section 2.6; Table 3 shows the dimension of each data array. DiBP and the IS (DiBP-d_4) overlap due to their similar structures, so they were recorded in the same chromatographic window.

The data arrays were decomposed using PARAFAC2 by applying the ALS algorithm with non-negativity constraints in the three ways. This multi-way technique was used because it makes discrimination between target compounds and unexpected interferents, which are those compounds that co-elute and share m/z ratios with the first ones, possible. The possibility of determining a compound in the presence of unknown interferents is called the second-order property. PARAFAC2 was used to model slight chromatographic peak shifts observed, but the second-order property is maintained if correlation between retention times is the same in all chromatograms [19]. In addition, if data are trilinear, the

Table 5
Experimental plan of the D-optimal design chosen for the optimization of the SPME.

Experiment	Block (day)	Type of fiber	Desorption time (min)	To add salt	Extraction temperature (°C)	Extraction time (min)
7	1	2	5	no	70	10
10	2	1	2	yes	70	10
24	2	2	5	no	80	10
25	1	1	2	yes	80	10
37	1	1	5	no	70	20
44	2	2	2	yes	70	20
50	2	1	2	no	80	20
63	1	2	5	yes	80	20
67	1	2	2	no	70	30
78	2	1	5	yes	70	30
81	1	1	2	no	80	30
96	2	2	5	yes	80	30
106	2	1	2	yes	70	40
117	1	1	5	no	80	40

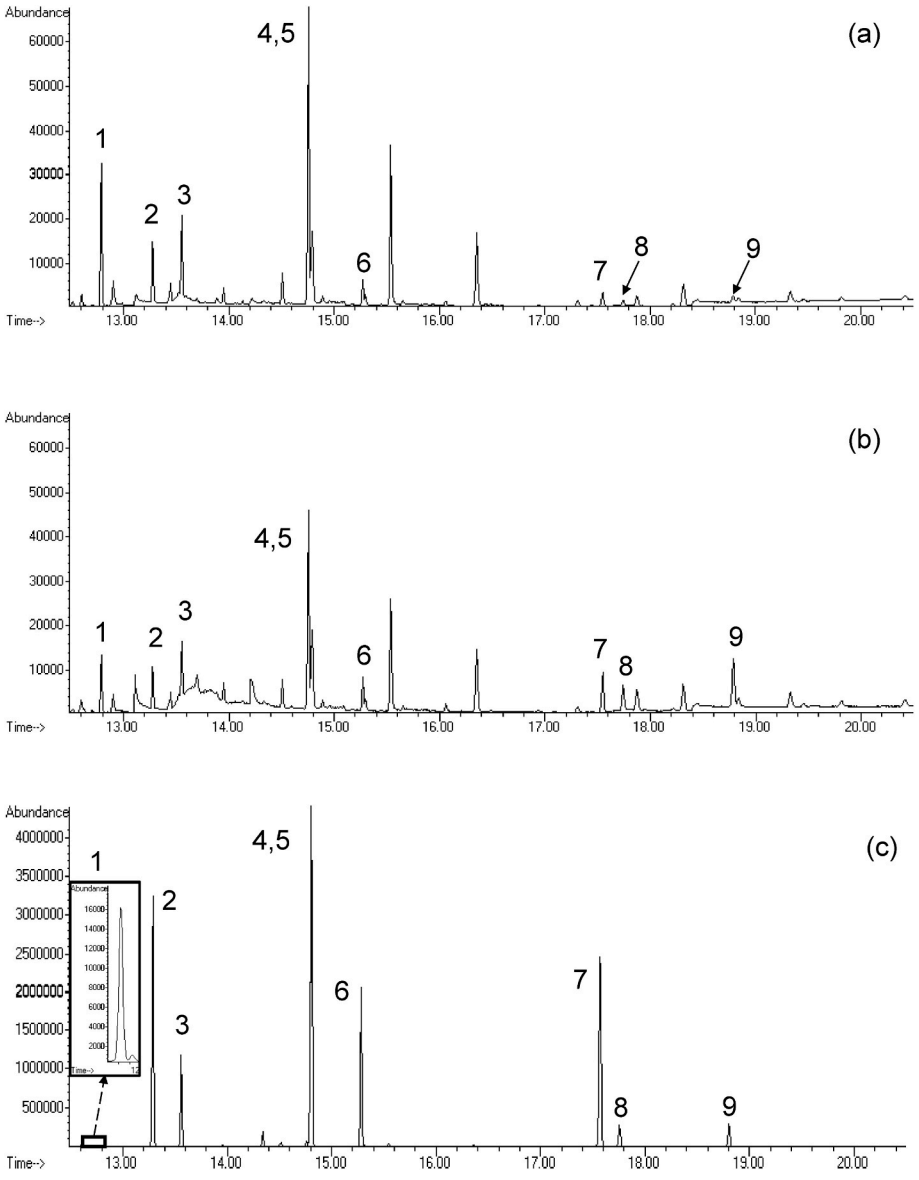

Fig. 1. Chromatograms obtained from solutions containing the same levels of analyte concentration. (a) Chromatogram of experiment 37 in Table 5 (fiber1; without addition of salt; desorption time: 5 min; extraction temperature: 70 °C; and extraction time: 20 min), (b) chromatogram of experiment 24 in Table 5 (fiber2; without addition of salt; desorption time: 5 min; extraction temperature: 80 °C; and extraction time: 10 min), and (c) chromatogram recorded in the chosen conditions (fiber 2; addition of salt; desorption time: 5 min; extraction temperature: 80 °C; and extraction time: 40 min). Analytes: 1 (BHT), 2 (DEP), 3 (BP), 4 (IS), 5 (DiBP), 6 (DBP), 7 (BBP), 8 (DEHA), 9 (DEHP).

chromatographic, spectral and sample profiles are obtained for each target compound due to the uniqueness property of this array decomposition. This also enables the unequivocal identification of target compounds, by means of their chromatographic and spectral profiles, according to official regulations and guidelines [50].

The PARAFAC2 models were built with different number of factors for each data array. After outlier detection, the chosen model in each case was that with higher explained variance and core consistency

diagnostic (CORCONDIA) values, and ensuring that the unequivocal identification of the corresponding compounds was successful. By way of example, the characteristics of the models built, with different number of factors for the data arrays of Day 1, are shown in Table S1 in the supplementary material. In general, in those cases where the compounds of interest are unequivocally identified, the models with higher explained variance and CORCONDIA values were chosen (this is the case of BP, DBP and DEHP). The model was considered invalid when CORCONDIA values are less than zero (then trilinearity is not fulfilled as shown in Ref. [51], as occur for DEP with 2 factors; BP, DBP and DEHP with 3 factors; and DiBP and IS with 4 factors, or when the unequivocal identification is not proper, as occurs for BHT, DiBP and IS, BBP and DEHA with 2 factors.

The number of factors and the explained variance of the final

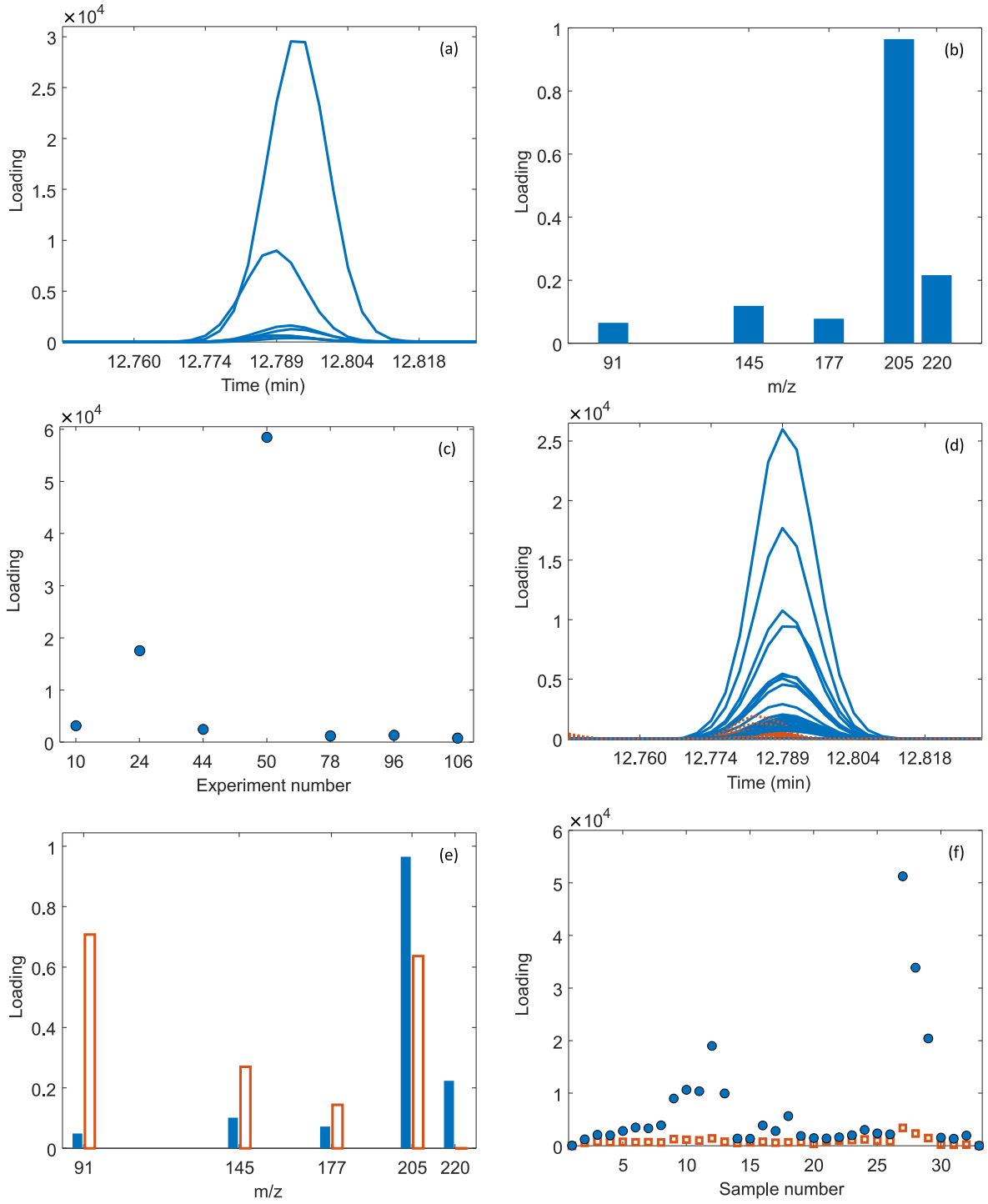

Fig. 2. Loadings of the chromatographic (a, d), spectral (b, e) and sample (c, f) modes of the PARAFAC2 models fitted for BHT: (a, b and c) in the optimization step (PARAFAC2 model calculated with experiments of day 2: experiments 10, 24, 44, 50, 78, 96 and 106 in Table 5); and (d, e and f) in the determination of commercial water samples (day 3 array: system blanks (samples 1 and 33), calibration standards (samples 2–13), standards at a fixed concentration were only the concentrations of IS varies (samples 14 and 15), replicates of a calibration standard (samples 16–20), sample D3_1 (samples 21–23), sample D3_2 (samples 24–26), sample D3_3 (samples 27–29), sample D3_3 diluted (samples 30–32)). First factor in solid blue, second factor in dashed/empty orange. (For interpretation of the references to colour in this figure legend, the reader is referred to the Web version of this article.)

PARAFAC2 models are shown in Table 3 (rows related to the experimental design). No outliers were found in any of the models built, being the confidence level for Q residual and Hotelling's T^2 indices 99% and 95%, respectively. Explained variance values above 99.8% were obtained in all cases. CORCONDIA [52] values > 99%, which imply appropriate models, were calculated in all cases. Three factors were required for the joint model built for DiBP and IS, and two factor models were obtained for BP, DBP and DEHP, which highlighted the need to use a decomposition method with the second order property such as PARAFAC2 to extract the part of the signals corresponding to unknown interferents in separate factors. The models for the remaining analytes were one factor models; Fig. 2 shows the loadings of the chromatographic (a), spectral (b) and sample (c) modes of the model fitted for BHT from experiments of day 2 (experiments 10, 24, 44, 50, 78, 96 and 106 in Table 5). In this case, it can be observed a small displacement in the chromatographic peaks (Fig. 2(a)).

In fact, before fitting the experimental design, it is necessary to guarantee that the loadings of the sample profiles, that will be used as responses, correspond unequivocally to the analytes and IS. In this work, their unequivocal identification was performed according to EUR 24105 EN [53]. To calculate the permitted tolerance intervals, the five reference standards were prepared and analysed by using the procedure described in section 2.5. The data were arranged in data arrays which were decomposed by using PARAFAC2; Table 3 (rows related to tolerance intervals) shows the characteristics of the corresponding arrays and models. Tolerance intervals for relative ion abundances were calculated according to the tolerances established in EUR 2410 EN [53], from the unique spectral profile provided by PARAFAC2 for each compound. Intervals for relative retention time were estimated with a margin of ±0.5%, according to the above regulation, from the corresponding chromatographic profiles. These tolerance intervals (see Table S2 in the supplementary material) were used throughout the paper to unequivocally identify the analytes in the PARAFAC2 models obtained from the different data array analysed.

The target analytes and IS were unequivocally identified in all 14 experiments of the D-optimal design since retention times and relative ion abundances of the corresponding chromatographic and spectral profiles from PARAFAC2 are inside the tolerance intervals in Table S2 in the supplementary material. At least 3 relative ion abundances were within the tolerance intervals for all the compounds, as EUR 2410 EN [53] requires for EI-GC-MS determinations.

The loadings of the sample profiles are proportional to concentration, so that the effect of the SPME conditions of the experiments on the quantitative determination of the target analytes may be assessed via the effect on the loading corresponding to the analytes, and ensuring that the analytes are unequivocally identified. For each compound, the loadings of the sample profile in Table 6 are the responses to be modelled through equation (2).

3.1.3. Model fitting

When fitting the models, it was possible to estimate the standard deviation of residuals and assess the significance of the fitted models since there were 14 experiments and 12 coefficients. On this basis, and noting the very wide range of the responses, the Box-Cox transformation [17,54] were taken as the response for the nine models. The transformation of each response variable and the coefficients and p-values of the test of the significance of the fitted models are shown in Table 7. All models were significant at 5% significance level except those fitted for DEHA and DEHP, which would be significant at a 11 and 12% significance levels. This is admissible because the residual standard deviation has only two degrees of freedom and this affect the validity of the significance tests of both the model and the coefficients.

3.1.4. Joint analysis of responses within the experimental domain

In order to explore the different HS-SPME conditions over the whole experimental domain, the responses were estimated for the 128 experiments of the full factorial design from the models in Table 7. The aim was to choose a HS-SPME conditions, among the 128 possible, that led simultaneously to the greatest value of the loadings of the sample profile (y_i, i = 1, …,9) associated to each analyte, resulting in a higher yield.

The strategy used was similar to that in reference [42]. The tools for the analysis are the parallel coordinates plots [21,55] and, in case of conflict between different experimental conditions for the SPME in that they were suitable for some analytes but for other they were not, the Pareto front [24] for the optimal solutions would be calculated.

The Box-Cox transformation for the first six response variables, y_i i = 1, …, 6, was an increasing monotone function of each of them, so the SPME conditions that maximize the transformation of the variable are the same that maximize the variable itself. On the contrary, the transformation of the last three responses, y_i i = 7, 8, 9, was a decreasing monotone function, thus the greater value of the response is reached with the SPME conditions that lead to the lower value of its transformation. The SPME conditions that simultaneously maximize the first six responses and minimize the last three had to be found, as the analysis was made with the models in Table 7 (transformed responses).

Once the value of each transformed response was calculated for each of the 128 experiments there was a vector of dimension nine ($\ln(y_1)$, $(y_2)^{0.3}$, $(y_3)^{0.4}$, $(y_4)^{0.6}$, $(y_5)^{0.5}$, $(y_6)^{0.1}$, $(y_7)^{-0.2}$, $(y_8)^{-0.18}$, $(y_9)^{-0.33}$) which described the conditions of each SPME. A Cartesian representation in 9 dimensions was not possible, so the parallel coordinates plot was used. In the plot, the values of each response are represented in vertical lines, and joining the values that correspond to one of the experiments, the vector ($\ln(y_1)$, $(y_2)^{0.3}$, …, $(y_9)^{-0.33}$) is represented by a broken line. The parallel coordinates plot with the effect of the 128 experiments on the transformed responses is shown in Fig. 3 (the levels of the six factors and their corresponding nine responses for the full design can be seen in Table S3 in the supplementary material). Maximum and minimum values for each response are shown because the responses have been set

Table 6
Responses (loadings of the sample profile of the PARAFAC2 models) for the 14 experiments of the D-optimal design.

Experiment	y_1 (BHT)	y_2 (DEP)	y_3 (BP)	y_4 (IS)	y_5 (DiBP)	y_6 (DBP)	y_7 (BBP)	y_8 (DEHA)	y_9 (DEHP)
7	15153	7673	8282	10228	21842	10740	7417	5051	8213
10	1076	264000	123600	49506	89385	46459	10894	994	1768
24	16092	9314	12393	10986	21566	13172	9766	5587	9666
25	913	238430	109220	59194	111170	53880	14420	3549	4338
37	50279	17694	17111	24386	46308	19592	6172	3339	7110
44	2278	269510	190850	106300	185880	124220	107540	9802	17763
50	53084	27051	28254	62109	100070	64554	18478	12427	12284
63	663	857210	383010	466670	773210	542420	569600	41185	48899
67	27784	23234	26733	41468	69776	33183	24539	21545	25340
78	615	745270	353900	404280	662930	403590	48110	3708	4491
81	67139	51005	47771	107380	180380	83099	27075	24057	19703
96	1016	1082600	547100	585910	965580	892760	1611700	271970	393910
106	506	824120	418410	644300	1042100	758110	134010	10511	10262
117	69233	74453	68008	178360	274140	149750	51375	121930	92718

Table 7
Box-Cox transformations and coefficients and p-values of the test of significance of the fitted models. The coefficients significantly different from zero at 5% significance level are in italics.

Coeff.	$\ln(y_1)$	$(y_2)^{0.3}$	$(y_3)^{0.4}$	$(y_4)^{0.6}$	$(y_5)^{0.5}$	$(y_6)^{0.1}$	$(y_7)^{-0.2}$	$(y_8)^{-0.18}$	$(y_9)^{-0.33}$
b_0	*8.629*	*37.589*	*108.600*	*1409.655*	*523.269*	*3.225*	*0.119*	0.180	*0.041*
b_{1A}	*−0.048*	0.077	−2.486	−6.961	1.500	−0.023	0.001	−0.004	−0.002
b_{2A}	*0.102*	0.170	*−3.019*	−32.517	−7.184	−0.015	*0.015*	0.024	*0.011*
b_{3A}	*0.281*	*−3.228*	*−9.680*	*−310.994*	*−90.711*	*−0.080*	0.000	−0.001	0.000
b_{4A}	*1.765*	*−16.025*	*−45.239*	*−565.186*	*−185.888*	*−0.300*	*0.021*	−0.000	−0.001
b_{5A}	*−0.262*	−1.362	*−4.363*	−42.484	−18.253	*−0.083*	*0.012*	0.025	0.008
b_{6A}	*−0.352*	*−9.212*	*−35.417*	*−933.083*	*−291.510*	*−0.472*	*0.038*	*0.056*	*0.020*
b_{6B}	*0.354*	−1.840	*−6.029*	*−225.246*	*−62.771*	−0.053	0.002	0.008	0.000
b_{6C}	*0.044*	*4.570*	*15.536*	*298.878*	*98.158*	*0.152*	*−0.010*	−0.015	−0.004
b_{5A6A}	*0.288*	1.461	*4.062*	21.135	9.875	0.059	*−0.008*	−0.009	−0.002
b_{5A6B}	*0.557*	*−3.694*	*−8.781*	*−408.841*	*−119.080*	*−0.130*	0.004	−0.002	−0.003
b_{5A6C}	*−0.084*	−1.707	*−7.381*	*−215.144*	*−63.996*	−0.060	0.003	0.006	0.003
p-value*	$<10^{-4}$	$5.31\ 10^{-3}$	$1.10\ 10^{-3}$	$1.14\ 10^{-3}$	$2.30\ 10^{-3}$	$5.98\ 10^{-3}$	$2.69\ 10^{-3}$	0.127	0.113

y_1: BHT; y_2: DEP; y_3: BP; y_4: IS; y_5: DiBP; y_6: DBP; y_7: BBP; y_8: DEHA; y_9: DEHP; (*) Test of significance of the model.

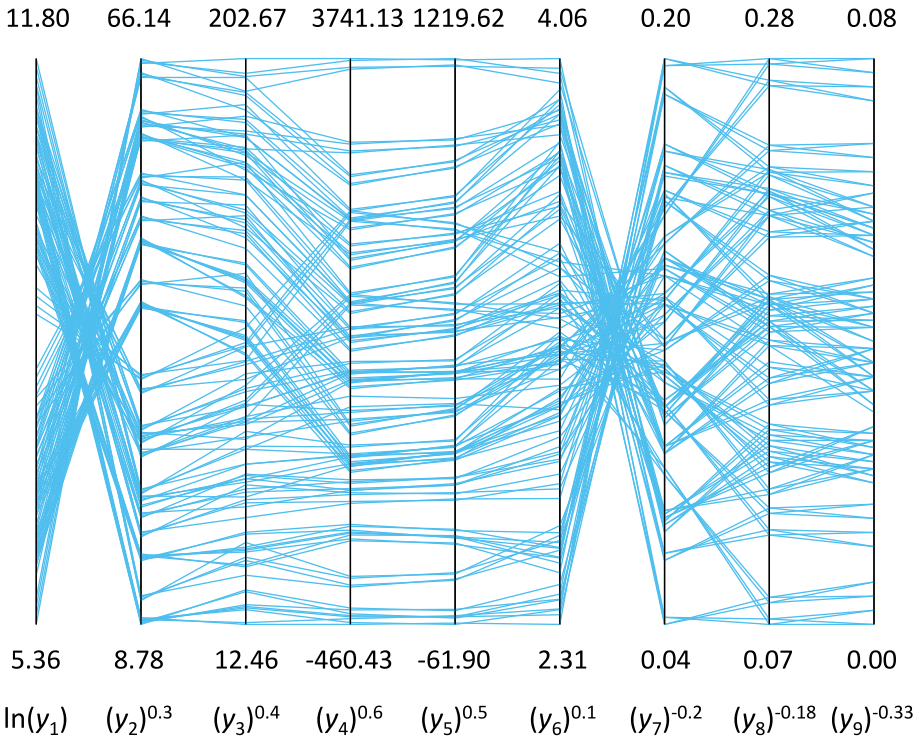

Fig. 3. Scaled parallel coordinates plot of the nine transformed responses for the 128 experiments of the full factorial design. Responses and analytes: y_1 (BHT), y_2 (DEP), y_3 (BP), y_4 (IS), y_5 (DiBP), y_6 (DBP), y_7 (BBP), y_8 (DEHA) and y_9 (DEHP).

on a common scale, with minimum 0 and maximum 1, to make the joint visualization of values possible.

Fig. 3 shows that the different SPME conditions have a similar effect on 4th and 5th responses because the segments that joint the values for both responses are parallel. This is consistent with the fact that the corresponding analytes are IS (DiBP-d_4) and DiBP, respectively. The opposite case, demonstrated through segments that intersect, is e.g. for 1st and 2nd variables, which are related to the effect on the extraction of BHT and DEP; SPME conditions that increase the extraction of BHT clearly have the opposite effect on DEP. In other cases, for example for 3rd and 4th responses, do not have this antagonistic effect for all the SPME conditions but just for a group of them. The same applies to the effect of SPME conditions on DEHA and DEHP, but in these cases it should be reminded that, due to the transformation of the original response, the maximum extraction is achieved for the lower values of the transformed responses.

It is at any rate clear that none of the conditions of the 128 experiments has simultaneously a high and positive effect on the responses of the 9 analytes. For that reason, a compromise has to be reached in order to choose the SPME conditions. To address this issue, it is helpful to consider just those SPME conditions that have the same effect on all analytes and are the best for at least one of them. The set of SPME procedures that fulfils this condition is the Pareto front of the 128 vectors formed from the 9 responses. The 40 vectors ($\ln(y_1)$, $(y_2)^{0.3}$, …, $(y_9)^{-0.33}$) contained in the Pareto front are shown in Fig. 4 (the levels of the factors related to these responses can be seen highlighted in yellow in Table S3 in the supplementary material). It has to be considered that none of them has extraction time shorter than 30 min; which excludes 64 experiments, i.e. half of the domain under study. That this, if a SPME with extraction time less than or equal to 20 min is used, a lower yield is achieved for at least one of the analytes. This is not the case for the rest of factors, e.g. extractions with and without addition of salt are in the Pareto front.

When comparing Figs. 3 and 4, it is observed that for all analytes,

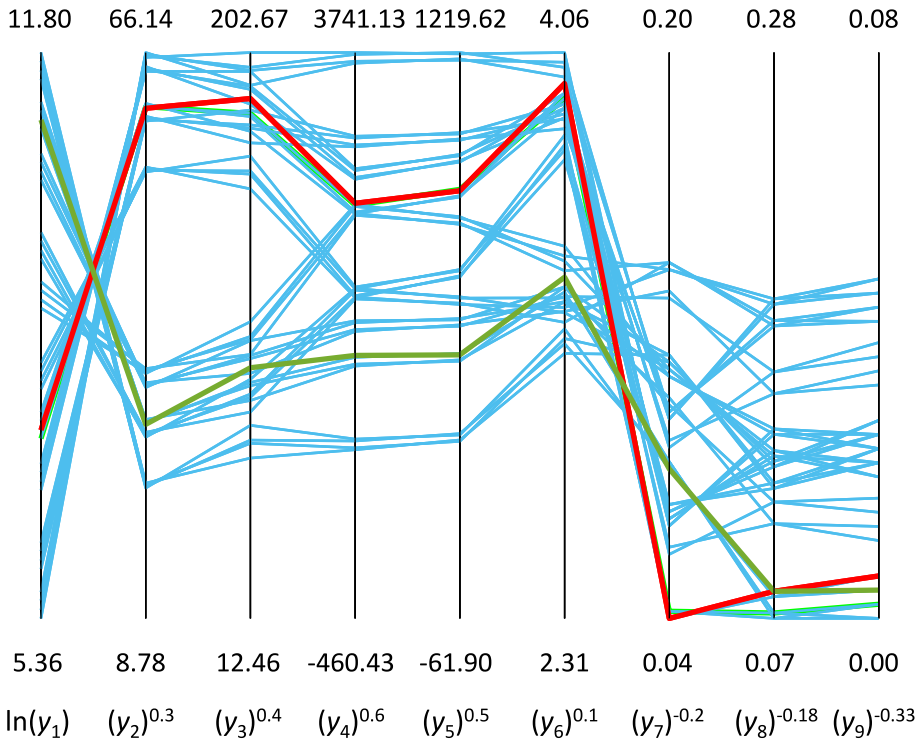

Fig. 4. Scaled parallel coordinates plot of the nine transformed responses for the 40 experiments of the Pareto-optimal front. The red line highlights the transformed responses expected from the SPME conditions chosen (fiber 2, 5 min of desorption time, addition of salt, 80 °C of extraction temperature and 40 min of extraction time). The green line highlights the responses expected when apply these same SPME conditions but with no addition of salt. Responses and analytes: y_1 (BHT), y_2 (DEP), y_3 (BP), y_4 (IS), y_5 (DiBP), y_6 (DBP), y_7 (BBP), y_8 (DEHA) and y_9 (DEHP). (For interpretation of the references to colour in this figure legend, the reader is referred to the Web version of this article.)

except BHT, the worst extractions are not a part of the Pareto front. On the contrary, the effect of extractions contained in the Pareto front are in the full range of the response related to BHT.

The SPME conditions chosen, red line in Fig. 4, kept the extraction of BBP, DEHA and DEHP close to the maximum, as well as that for DBP, DEP and BP, and slightly lower for DiBP and IS. It should also be noted that if the SPME conditions that lead to the maximum extraction for these last five analytes would have been chosen, a minimum extraction had been for BHT. Whichever of the extraction procedures related to the maximum yield for BHT led to much worse values for the rest of the analytes. The final conditions were: using fiber 2 (50/30 μm DVB/CAR/PDMS), 5 min of desorption time, addition of salt, and temperature and time of extraction, 80 °C and 40 min, respectively.

Fig. 1(c) shows the chromatogram recorded from the final SPME conditions chosen. Clearly, in the extraction conditions obtained from the developed procedure the higher sensitivity was achieved for all the target compounds but BHT; it should be noted that the maximum abscissae for plot (c), chromatogram obtained in the chosen conditions, and those for plots (a) and (b) differ by two orders of magnitude. Changing the level of the block factor (day) by maintaining the remaining factors at the chosen levels had a completely negligible influence on the extraction of all compounds; nevertheless, without the addition of salt, all extractions got notably worse except for BHT, for which the yield of extraction was increased, as green line in Fig. 4 shows.

3.2. Some figures of merit of the analytical procedure

With the aim of characterizing the analytical procedure, some figures of merit were determined: linear dynamic range, accuracy (trueness and precision), critical value of the concentration and minimum detectable value of the concentration. Firstly, a set of 14 standards and 2 system blanks were injected, in accordance with the procedure described in section 2.5 with the final SPME conditions chosen in section 3.1.4, for establishing the linear dynamic range. On completion of the chromatographic analysis, data were arranged in data arrays and then the PARAFAC2 models detailed in Table 3 (rows related to the linear dynamic range) were built which explained variances greater than 99.6% with CORCONDIA index equal to 100 in all cases. The unequivocal identification of the compounds was carried out as in section 3.1.2. In this case, as for the remainder of the paper, the standardized sample loadings, i.e. sample loadings of the target analytes divided by the loadings IS, were considered.

Linear regression models between the standardized loadings of the sample mode of the PARAFAC2 and the analyte concentration were fitted; outliers, data with absolute value of standardized residue greater than 2.5, were previously found using the least trimmed squares (LTS) regression [56] and removed. The linear dynamic ranges found for the different target analytes are shown in Table 8. The corresponding accuracy lines were used to assess trueness and precision; the parameters in Table 8 are that of the least squares regression models fitted for the different analytes. The correlation coefficients of the latter regressions are the same as those of the corresponding models obtained when estimating the linear dynamic range.

Trueness was determined by checking the p-value to joint hypotheses test "H_0: the intercept of the accuracy line is 0 and the slope is 1". In all cases, the values were higher than 0.05 so there is no evidence to reject the null hypothesis, i.e. intercept and slope are zero and unity respectively, therefore it was concluded that no bias was present in any of the determinations. The standard deviation of regression (s_{yx} in Table 8) is an estimate of the intermediate precision of the analytical method for each target compound.

The critical value of the concentration (x_C) and minimum detectable value of the concentration (x_D) were estimated according to ISO 11843 [57] by using the method proposed in Ref. [58], based in three calibration lines carried out in three different days and fitted in a reduced range of concentrations (from 0 to 1.0 μg L^{-1} for BHT, to 12.5 μg L^{-1} for DEP, to 2.5 μg L^{-1} for BP, to 5 μg L^{-1} for DiBP, to 3 μg L^{-1} for DBP, to 30 μg L^{-1} for BBP, to 50 μg L^{-1} for DEHA and to 40 μg L^{-1} for DEHP). The details about the corresponding PARAFAC2 models are shown in Table 3. The values estimated for both figures of merit are shown in Table 8. The analytical procedure allows to detect up to 0.26 μg L^{-1} of BP, and 9.69 μg L^{-1} in the case of DEHP, with a probability of false positive set at 0.05.

Finally, eight (five for the highest concentration level) fortified blank

Table 8
Figures of merit of the analytical procedure.

Analyte	Linear range (μg L^{-1})	Accuracy line					x_C (μg L^{-1})	x_D (μg L^{-1})
		Intercept	Slope	r	s_{yx} (μg L^{-1})	p-value		
BHT	0–1	−0.002	1.003	0.995	0.047	0.806	0.36	0.69
DEP	0–12.5	0.001	1.000	0.999	0.195	1.000	0.65	1.27
BP	0–2.5	0.000	1.000	0.997	0.085	1.000	0.26	0.51
DiBP	0–5	−0.001	1.001	0.999	0.066	0.999	0.40	0.79
DBP	0–5	−0.001	1.000	0.985	0.372	1.000	0.27	0.53
BBP	0–250	−0.001	1.000	0.988	16.04	1.000	3.65	7.06
DEHA	0–250	0.002	1.000	0.989	20.20	1.000	6.36	12.35
DEHP	0–500	−0.008	1.000	0.991	36.23	1.000	9.69	18.30

r: correlation coefficient; s_{yx}: standard deviation of regression; p-value to jointly test the intercept = 0 and slope = 1; x_C: critical value of the concentration (α = 0.05); x_D: minimum detectable value of the concentration (α = β = 0.05).

samples at three levels of concentration for each analyte were measured in three different days. These data were included to study the location and dispersion of the measurements. The robust standard deviation (rSD) was calculated by means of: rSD = MAD*1.4826. MAD is the median absolute deviation which is estimated based on the median absolute deviation (the median of the absolute differences between each data value and the median of the population) [59]. In addition, the robust coefficient of variation (rCV) was calculated. These values are shown in Table 9. In general, the best values of rCV appear for the higher true concentration.

3.3. Analysis of bottled natural mineral water samples

Lastly, the target analytes were determined in the 9 bottled water samples in Table 1, involving different types of waters in different types of packaging. The samples were analysed, in triplicate, over 3 days. The corresponding data arrays, together with the characteristics of the PARAFAC2 models, are shown in Table 3 (rows related to the bottled water analysis). The PARAFAC2 models explain variances greater than 99.5%, with CORCONDIA indices equal to 100, in all cases.

By way of example, Fig. 2(d–f) show the loadings of the chromatographic, spectral and sample modes of the two factor PARAFAC2 model built for BHT from the data set of day 3. The first factor (in blue) was unequivocally identified as that corresponding to BHT since both the relative abundances and relative retention times, estimated from the spectral and chromatographic modes, were inside the corresponding tolerance intervals (these intervals are shown in the last columns in Table S2 in the supplementary material). The second factor (in orange) was related to an unknown interferent. This is a clear example of the advantage of using the multi-way technique; as can be seen in Fig. 2, the interferent appear both in the chromatographic (Fig. 2(d)) and spectral modes (Fig. 2(e)), so its presence in the sample could have cause false negative during BHT identification. The loadings of the sample mode of the second factor do not increase with the concentration of BHT for the calibration standards (samples 2–13, Fig. 2(f)), which support the fact that the factor was not related to this target compound.

Table 9
Location and scale robust estimates for the measurements of eight replicates at three levels of concentration for each analyte (five for the highest concentration level).

Analyte	C_{true} (μg L^{-1})	Median (μg L^{-1})	rSD (μg L^{-1})	rCV (%)
BHT	0.2*	–	–	–
	0.4*	–	–	–
	0.6*	–	–	–
DEP	0.8*	–	–	–
	2.5	2.79	1.20	43.01
	10	10.89	1.10	10.07
BP	0.3*	–	–	–
	0.5*	–	–	–
	2	1.18	0.19	8.84
DiBP	2	1.75	0.16	9.32
	3	3.07	0.20	6.51
	4.5	4.55	0.030	0.65
DBP	0.8	0.74	0.13	17.03
	1.2	1.12	0.12	10.59
	2.5	2.57	0.074	2.88
BBP	5*	–	–	–
	12.5	12.41	1.08	8.66
	20	20.99	8.09	38.53
DEHA	10*	–	–	–
	20	20.08	8.24	41.05
	40	21.11	7.78	36.87

C_{true}, true concentration; rSD robust standard deviation; rCV, robust coefficient of variation, rCV (%) = (rSD/median) × 100; (*) the concentrations were below the minimum detectable value of the concentration.

Most of the concentrations of the target analytes found in the bottled water samples in Table 1 were statistically equal to zero or below the minimum detectable value of the concentration (x_D). BHT was found in sample D3_3, which was analysed from three different bottles. In the last bottle a concentration of 1.05 μg L^{-1} was found, whereas in the other two bottles the concentrations were over the calibration range (the standardized loadings can be seen in Fig. S1 in the supplementary material). The values of BHT found may be attributed to the metal cap used in the packaging of that sample; residues of similar compounds have been found in this type of packing [60]. As is mentioned above, Fig. 2(f) shows the loadings of the sample mode for BHT. Samples from 21 to 29 are the loadings of the 3 last commercial brands in Table 1. The loadings of the samples 27–29 (sample D3_3), while they have not yet been standardized, were over the range of calibration (high chromatographic peaks were detected in the experimental session), for that reason, sample D3_3 was diluted (samples 30–32) were analysed too.

Nevertheless, the concentrations found for the target analytes in the bottled water samples analysed in this work were really low, that is, the compounds are not present in quantities that may be injurious to human health.

4. Conclusions

Using a D-optimal design, 14 experiments, among the 128 of the full factorial design, were sufficient to estimate the mathematical models that related the responses to the effect of the experimental factors on the extraction of the considered compound. As a result, a very significant reduction in the experimental effort required by the study as well as in its cost was achieved.

The methodology developed has led to find the conditions for the six HS-SPME experimental factors considered that jointly satisfied the requirements of eight different target analytes in order to increase the efficiency of the extraction procedure. The use of the Pareto front and parallel coordinates greatly helped to effectively address the multi-objective optimization.

PARAFAC2 decomposition has allowed the coelution of interferents that share *m/z* ratios with the target analytes to be successfully addressed. Consequently, it has been possible to unequivocally identify the latter, according to EUR 2410 EN, thereby avoiding to cause possible

false negative results due to a mistake in the identification of them because of the interferents.

Null or below the minimum detectable value of the concentrations have been found for all the target analytes except for BHT, which was found in three of the bottled natural water analysed with metal cap, but at so low levels that do not pose any risk to human health.

Annex

$\underline{\mathbf{X}}$ is a data cube of dimension $I \times J \times K$ where I is the number of elution times, J the number of values of the recorded spectrum at each time (e.g. the number of wavelengths in HPLC-DAD or the m/z ratios in GC-MS) and K the number of samples analysed. The structural model for PARAFAC with F factors is given by equation (A1) for each one of the matrices which forms the cube $\underline{\mathbf{X}}$.

$$\mathbf{X}_k = \mathbf{B}\mathbf{D}_k\mathbf{A}^{\mathrm{T}} + \mathbf{E}_k \quad k = 1, \ldots, K \tag{A1}$$

$\mathbf{B}$ is a $I \times F$ matrix which columns are the elution profiles common to the K samples. $\mathbf{D}_k$ is a $F \times F$ diagonal matrix which contain the contribution to the k-th sample of the F factors (analytes). $\mathbf{A}$ is a $J \times F$ matrix which contains the spectral profiles of the F analytes that are also common in all the samples. Finally, $\mathbf{E}_k$ is the k-th residual $I \times J$ matrix.

The structural model in equation (A1) is a trilinear model. Unlike the bilinear structural models, it has not rotational ambiguity and so the solution is unique. This guarantees that the PARAFAC decomposition of $\underline{\mathbf{X}}$ provides the elution and spectral profiles of the compounds present in the analysed samples, making it possible the unequivocal identification of them by two independent ways. In addition, it provides the second-order property: analytes may be quantified in the presence of co-eluent not present in the calibration standards.

When retention time shifts occur, equation (A1) is no longer suitable for $\underline{\mathbf{X}}$, and there is equation (A2) instead.

$$\mathbf{X}_k = \mathbf{B}_k\mathbf{D}_k\mathbf{A}^{\mathrm{T}} + \mathbf{E}_k \quad k = 1, \ldots, K \tag{A2}$$

$\mathbf{B}_k$ remains a $I \times F$ matrix which columns are the F elution profiles in the k-th sample, because of the shift change from one sample to another.

Between laying down that all the $\mathbf{B}_k$ are equal, as PARAFAC model does, and admit that all are different without no relationship among them, there is the possibility of introducing constraints. It is particularly relevant the case in which it is imposed that the cross-product of the matrix is equal for all k, equation (A3).

$$\mathbf{B}_k^{\mathrm{T}}\mathbf{B}_k = \mathbf{B}^{\mathrm{T}}\mathbf{B} \quad k = 1, \ldots, K \tag{A3}$$

The structural model in equation (A2) with the constrain in equation (A3) is PARAFAC2 and it has unique solution and therefore the second-order property.

Then, we will show that when there is a shift of the elution profile, the constrain of equation (A3) is fulfilled. The F elution profiles in the sample k-th would be formally given by equation (A4).

$$\mathbf{B}_k = \left({}^k\mathbf{b}_1, {}^k\mathbf{b}_2, \ldots, {}^k\mathbf{b}_F\right) \quad k = 1, \ldots, K \tag{A4}$$

It may be assumed that the F profiles have the same shift in the k-th sample and that, in the acquisition window, the elution base line is represented both before and after all analytes appear. Taking the $\mathbf{B}_1$ profiles as a reference, which is not a loss of generality, and assuming that a shift to the right of L time units occurs for k-th sample, there is

$$\mathbf{b}_f{}^k = \mathbf{P}^T\mathbf{b}_f{}^1 \quad f = 1, \ldots, F \text{ with } \quad \mathbf{P}_{I\times I} = \left(\begin{array}{c|c} \mathbf{0}_{(I-L)\times L} & \mathbf{I}_{I-L} \\ \hline \mathbf{I}_L & \mathbf{0}_{L\times(I-L)} \end{array}\right) \tag{A5}$$

Being $\mathbf{P}$ the $I \times I$ matrix formed by the unity matrices with dimension L and I-L and the rectangular matrices formed by ceros. The columns of P are orthogonal two by two and with norm 1, for that reason it is an orthonormal matrix and $\mathbf{P}^T\mathbf{P} = \mathbf{P}\mathbf{P}^T = \mathbf{I}$ is fulfilled. If the shift had been to the left, the matrix in equation (A5) would be $\mathbf{P}^T$.

When you consider equation (A5), the cross-product matrix of the elution profiles of the k-th sample, using the dot product, is written as:

$$\mathbf{B}_k^{\mathrm{T}}\mathbf{B}_k = \left({}^k\mathbf{b}_f^T \cdot {}^k\mathbf{b}_g\right) = \left(\left(\mathbf{b}_f^T{}^1\mathbf{P}\right) \cdot \left(\mathbf{P}^T\mathbf{b}_g{}^1\right)\right) = \left({}^1\mathbf{b}_f^T \cdot {}^1\mathbf{b}_g\right) = \mathbf{B}_1^{\mathrm{T}}\mathbf{B}_1 \tag{A6}$$

It is clear that the shifts do not need to be of equal length L from one matrix to another, not even in the same direction, but always the constrain in equation (A3) is fulfilled.

This means that theoretically the PARAFAC2 structural model is suitable for chromatographic data with shifts in the elution profile.

Credit author statement

L. Valverde-Som: Conceptualization, Methodology, Formal analysis, Investigation, Writing - Original Draft, Writing - Review & Editing, Visualization. **A. Herrero:** Conceptualization, Methodology, Formal analysis, Writing - Original Draft, Writing - Review & Editing. **C. Reguera:** Conceptualization, Methodology, Investigation, Writing - Review & Editing. **L.A. Sarabia:** Conceptualization, Methodology, Software, Formal analysis, Writing - Original Draft, Writing - Review & Editing, Visualization, Supervision. **M.C. Ortiz:** Conceptualization, Methodology, Writing - Review & Editing, Visualization, Supervision, Funding acquisition.

Abbreviations: 2,6-di-tert-butyl-4-methyl-phenol (BHT), benzophenone (BP), benzyl butyl phthalate (BBP), bis(2-ethylhexyl) adipate (DEHA), bis(2-ethylhexyl) phthalate (DEHP), carboxen® (CAR), core consistency diagnostic (CORCONDIA), critical value of the concentration (x_C), dibutyl phthalate (DBP), diethyl phthalate (DEP), diisobutyl phthalate (DiBP), diisobutyl phthalate-3, 4, 5, 6-d_4 (DiBP-d_4), divinylbenzene (DVB), electron impact (EI), head space-solid phase microextraction-gas chromatography-mass spectrometry (HS-SPME-GC-MS), internal standard (IS), mean absolute deviation (MAD), minimum detectable value of the concentration (x_D), parallel factor analysis (PARAFAC), polydimethylsiloxane (PDMS), polyethylene terephthalate (PET), probability of false positive (α), probability of false negative (β), recycled PET (RPET), robust coefficient of variation (rCV), robust standard deviation (rSD), variance inflation factor (VIF).

Declaration of competing interest

The authors declare that they have no known competing financial interests or personal relationships that could have appeared to influence the work reported in this paper.

Data availability

No data was used for the research described in the article.

Acknowledgments

The authors thank the financial support provided by Consejería de la Junta de Castilla y León (JCyL) through project BU052P20 co-financed with European FEDER funds. Lucía Valverde-Som thanks JCyL for her postdoctoral contract through this project.

Appendix A. Supplementary data

Supplementary data to this article can be found online at https://doi.org/10.1016/j.talanta.2022.124021.

References

[1] J. Pawliszyn, Handbook of Solid Phase Microextraction, Elsevier, Amsterdam, 2012, https://doi.org/10.1016/C2011-0-04297-7.
[2] V. Jalili, A. Barkhordari, A. Ghiasvand, A comprehensive look at solid-phase microextraction technique: a review of reviews, Microchem. J. 152 (2020), 104319, https://doi.org/10.1016/j.microc.2019.104319.

[3] C. Zambonin, A. Aresta, Recent applications of solid phase microextraction coupled to liquid chromatography, Sep 8 (2021) 34, https://doi.org/10.3390/separations8030034.

[4] W. Wardencki, M. Michulec, J. Curyło, A review of theoretical and practical aspects of solid-phase microextraction in food analysis, Int. J. Food Sci. Technol. 39 (2004) 703–717, https://doi.org/10.1111/j.1365-2621.2004.00839.x.

[5] S. Risticevic, H. Lord, T. Górecki, C.L. Arthur, J. Pawliszyn, Protocol for solid-phase microextraction method development, Nat. Protoc. 5 (2010) 122–139, https://doi.org/10.1038/nprot.2009.179.

[6] S. Wei, X. Xiao, L. Wei, L. Li, G. Li, F. Liu, J. Xie, J. Yu, Y. Zhong, Development and comprehensive HS-SPME/GC–MS analysis optimization, comparison, and evaluation of different cabbage cultivars (Brassica oleracea L. var. capitata L.) volatile components, Food Chem. 340 (2021), 128166, https://doi.org/10.1016/j.foodchem.2020.128166.

[7] L. Rubio, S. Sanllorente, L.A. Sarabia, M.C. Ortiz, Optimization of a headspace solid-phase microextraction and gas chromatography/mass spectrometry procedure for the determination of aromatic amines in water and in polyamide spoons, Chemometr. Intell. Lab. Syst. 133 (2014) 121–135, https://doi.org/10.1016/j.chemolab.2014.01.013.

[8] D. Granato, V.M. de Araújo Calado, The use and importance of design of experiments (DOE) in process modelling in food science and technology, in: D. Granato, G. Ares (Eds.), Mathematical and Statistical Methods in Food Science and Technology, John Wiley & Sons, Chichester, 2014, pp. 3–18, https://doi.org/10.1002/9781118434635.ch01.

[9] S.L.C. Ferreira, M.M. Silva Junior, C.S.A. Felix, D.L.F. da Silva, A.S. Santos, J. H. Santos Neto, C.T. de Souza, R.A. Cruz Junior, A.S. Souza, Multivariate optimization techniques in food analysis - a review, Food Chem. 273 (2019) 3–8, https://doi.org/10.1016/j.foodchem.2017.11.114.

[10] G. Marrubini, S. Dugheri, G. Cappelli, G. Arcangeli, N. Mucci, P. Appelblad, C. Melzi, A. Speltini, Experimental designs for solid-phase microextraction method development in bioanalysis: a review, Anal. Chim. Acta 1119 (2020) 77–100, https://doi.org/10.1016/j.aca.2020.04.012.

[11] S.T. Narenderan, S.N. Meyyanathan, V.V.S.R. Karri, Experimental design in pesticide extraction methods: a review, Food Chem. 289 (2019) 384–395, https://doi.org/10.1016/j.foodchem.2019.03.045.

[12] S. Pati, M. Tufariello, P. Crupi, A. Coletta, F. Grieco, I. Losito, Quantification of volatile compounds in wines by HS-SPME-GC/MS: critical issues and use of multivariate statistics in method optimization, Processes 9 (2021) 662, https://doi.org/10.3390/pr9040662.

[13] A. Biancolillo, R. Aloia, L. Rossi, A.A. D'Archivio, Organosulfur volatile profiles in Italian red garlic (*Allium Sativum* L.) varieties investigated by HS-SPME/GC-MS and chemometrics, Food Control 131 (2022), https://doi.org/10.1016/j.foodcont.2021.108477, 108477.

[14] J.M. Muñoz-Redondo, M.J. Ruiz-Moreno, B. Puertas, E. Cantos-Villar, J. M. Moreno-Rojas, Multivariate optimization of headspace solid-phase microextraction coupled to gas chromatography-mass spectrometry for the analysis of terpenoids in sparkling wines, Talanta 208 (2020), 120483, https://doi.org/10.1016/j.talanta.2019.120483.

[15] J. Pico, E.M. Gerbrandt, S.D. Castellarin, Optimization and validation of a SPME-GC/MS method for the determination of volatile compounds, including enantiomeric analysis, in northern highbush blueberries (*Vaccinium corymbosum* L.), Food Chem. 368 (2022), 130812, https://doi.org/10.1016/j.foodchem.2021.130812.

[16] A.C. Vieira, A.C. Pereira, J.C. Marques, M.S. Reis, Multi-target optimization of solid phase microextraction to analyse key flavour compounds in wort and beer, Food Chem. 317 (2020), 126466, https://doi.org/10.1016/j.foodchem.2020.126466.

[17] L.A. Sarabia, M.C. Ortiz, M.S. Sánchez, Response surface methodology, in: 2ª Ed., in: S. Brown, R. Tauler, B. Walczak (Eds.), Comprehensive Chemometrics. Chemical and Biochemical Data Analysis, vol. 1, Elsevier, 2020, pp. 287–326, https://doi.org/10.1016/B978-0-12-409547-2.14756-0.

[18] A. Herrero, S. Sanllorente, C. Reguera, M.C. Ortiz, L.A. Sarabia, A new multiresponse optimization approach in combination with a D-Optimal experimental design for the determination of biogenic amines in fish by HPLC-FLD, Anal. Chim. Acta 945 (2016) 31–38, https://doi.org/10.1016/j.aca.2016.10.001.

[19] A. Herrero, M.C. Ortiz, L.A. Sarabia, D-optimal experimental design coupled with parallel factor analysis 2 decomposition a useful tool in the determination of triazines in oranges by programmed temperature vaporization–gas chromatography–mass spectrometry when using dispersive-solid phase extraction, J. Chromatogr. A 1288 (2013) 111–126, https://doi.org/10.1016/j.chroma.2013.02.088.

[20] A. Herrero, C. Reguera, M.C. Ortiz, L.A. Sarabia, Determination of dichlobenil and its major metabolite (BAM) in onions by PTV-GC-MS using PARAFAC2 and experimental design methodology, Chemometr. Intell. Lab. Syst. 133 (2014) 92–108, https://doi.org/10.1016/j.chemolab.2013.12.001.

[21] M. Bystrzanowska, M. Tobiszewski, Multi-objective optimization of microextraction procedures, TrAC Trends Anal. Chem. 116 (2019) 266–273, https://doi.org/10.1016/j.trac.2018.12.031.

[22] G.C. Derringer, R. Suich, Simultaneous optimization of several response variables, J. Qual. Technol. 12 (1980) 214–219, https://doi.org/10.1080/00224065.1980.11980968.

[23] R. Morales, L.A. Sarabia, M.S. Sánchez, M.C. Ortiz, Experimental design for the optimization of the derivatization reaction in determining chlorophenols and chloroanisoles by headspace-solid-phase microextraction–gas chromatography/mass spectrometry, J. Chromatogr. A 1296 (2013) 179–195, https://doi.org/10.1016/j.chroma.2013.04.038.

[24] K. Deb, Multi-objective Optimization Using Evolutionary Algorithms, Wiley, 2001.

[25] M.C. Ortiz, L.A. Sarabia, A. Herrero, M.S. Sánchez, Vectorial optimization as a methodogical alternative to desirability function, Chemometr. Intell. Lab. Syst. 83 (2006) 157–168, https://doi.org/10.1016/j.chemolab.2005.11.005.

[26] R. Bro, PARAFAC. Tutorial and applications, Chemometr. Intell. Lab. Syst. 38 (1997) 149–171, https://doi.org/10.1016/S0169-7439(97)00032-4.

[27] H.A.L. Kiers, J.M.F. ten Berge, R. Bro, PARAFAC2-Part I. A direct fitting algorithm for the PARAFAC2 model, J. Chemom. 13 (1999) 275–294, https://doi.org/10.1002/(SICI)1099-128X(199905/08)13:3/4%3C275::AID-CEM543%3E3.0.CO;2-B.

[28] R. Bro, C.A. Andersson, H.A.L. Kiers, PARAFAC2-Part II. Modeling chromatographic data with retention time shifts, J. Chemom. 13 (1999) 295–309, https://doi.org/10.1002/(SICI)1099-128X(199905/08)13:3/4<295::AID-CEM547>3.0.CO;2-Y.

[29] M.C. Ortiz, L.A. Sarabia, M.S. Sánchez, A. Herrero, S. Sanllorente, C. Reguera, Usefulness of PARAFAC for the quantification, identification, and description of analytical data, in: A. Muñoz de la Peña, H.C. Goicoechea, G.M. Escandar, A. C. Olivieri (Eds.), Fundamentals and Analytical Applications of Multiway Calibration, Elsevier, Amsterdam, 2015, pp. 37–81, https://doi.org/10.1016/B978-0-444-63527-3.00002-3.

[30] R. Morales, M.C. Ortiz, L.A. Sarabia, Usefulness of a PARAFAC decomposition in the fiber selection procedure to determine chlorophenols by means SPME-GC-MS, Anal. Bioanal. Chem. 403 (2012) 1095–1107, https://doi.org/10.1007/s00216-011-5545-7.

[31] D. Arroyo, M.C. Ortiz, L.A. Sarabia, Optimization of the derivatization reaction and the solid-phase microextraction conditions using a D-optimal design and three-way calibration in the determination of non-steroidal anti-inflammatory drugs in bovine milk by gas chromatography-mass spectrometry, J. Chromatogr. A 1218 (2011) 4487–4497, https://doi.org/10.1016/j.chroma.2011.05.010.

[32] R. Morales, M.C. Ortiz, L.A. Sarabia, Optimization of headspace experimental factors to determine chlorophenols in water by means of headspace solid-phase microextraction and gas chromatography coupled with mass spectrometry and parallel factor analysis, Anal. Chim. Acta 754 (2012) 20–30, https://doi.org/10.1016/j.aca.2012.10.003.

[33] R. Tauler, Multivariate curve resolution applied to second order data, Chemometr. Intell. Lab. Syst. 30 (1995) 133–146, https://doi.org/10.1016/0169-7439(95)00047-X.

[34] A. de Juan, R. Tauler, Multivariate Curve Resolution: 50 years addressing the mixture analysis problem – a review, Anal. Chim. Acta 1145 (2021) 59–78, https://doi.org/10.1016/j.aca.2020.10.051.

[35] A.C. Olivieri, R. Tauler, N-BANDS, A new algorithm for estimating the extension of feasible bands in multivariate curve resolution of multicomponent systems in the presence of noise and rotational ambiguity, J. Chemom. 35 (2021) e3317, https://doi.org/10.1002/cem.3317.

[36] A.C. Olivieri, Evaluation of the ambiguity in second-order analytical calibration based on multivariate curve resolution. A tutorial, Microchem. J. 179 (2022), https://doi.org/10.1016/j.microc.2022.107455, 107455.

[37] H. Abdollahi, R. Tauler, Uniqueness and rotation ambiguities in multivariate curve resolution methods, Chemometr. Intell. Lab. Syst. 108 (2011) 100–111, https://doi.org/10.1016/j.chemolab.2011.05.009.

[38] H. Piri-Moghadam, F. Ahmadi, J. Pawliszyn, A critical review of solid phase microextraction for analysis of water samples, TrAC Trends Anal. Chem. 85 (2016) 133–143, https://doi.org/10.1016/j.trac.2016.05.029.

[39] N. Lorenzo-Parodi, W. Kaziur, N. Stojanovi, M.A. Jochmann, T.C. Schmidt, Solventless microextraction techniques for water analysis, TrAC Trends Anal. Chem. 113 (2019) 321–331, https://doi.org/10.1016/j.trac.2018.11.013.

[40] A. Guart, F. Bono-Blay, A. Borrell, S. Lacorte, Effect of bottling and storage on the migration of plastic constituents in Spanish bottled waters, Food Chem. 156 (2014) 73–80, https://doi.org/10.1016/j.foodchem.2014.01.075.

[41] F. Cincotta, A. Verzera, G. Tripodi, C. Condurso, Non-intentionally added substances in PET bottled mineral water during the shelf-life, Eur. Food Res. Technol. 244 (2018) 433–439, https://doi.org/10.1007/s00217-017-2971-6.

[42] M.M. Arce, S. Sanllorente, M.C. Ortiz, L.A. Sarabia, Easy-to-use procedure to optimise a chromatographic method. Application in the determination of bisphenol-A and phenol in toys by means of liquid chromatography with fluorescence detection, J. Chromatogr. A 1534 (2018) 93–100, https://doi.org/10.1016/j.chroma.2017.12.049.

[43] L.A. Sarabia, M.C. Ortiz, DETARCHI: a program for detection limits with specified assurance probabilities and characteristic curves of detection, TrAC Trends Anal. Chem. 13 (1994) 1–6, https://doi.org/10.1016/0165-9936(94)85052-6.

[44] R. Perestrelo, C.L. Silva, M. Algarra, J.S. Câmara, Monitoring phthalates in table and fortified wines by headspace solid-phase microextraction combined with gas chromatography-mass spectrometry analysis, J. Agric. Food Chem. 68 (2020) 8431–8437, https://doi.org/10.1021/acs.jafc.0c02941.

[45] L. Carnol, C. Schummer, G. Moris, Quantification of six phthalates and one adipate in Luxembourgish beer using HS-SPME-GC/MS, Food Anal. Methods 10 (2017) 298–309, https://doi.org/10.1007/s12161-016-0583-6.

[46] C. Domeño, M. Aznar, C. Nerín, F. Isella, M. Fedeli, O. Bosetti, Safety design of printed multilayer materials intended for food packaging, Food Addit. Contam. 34 (2017) 1239–1250, https://doi.org/10.1080/19440049.2017.1322221.

[47] E. Asensio, L. Montañés, C. Nerín, Migration of volatile compounds from natural biomaterials and their safety evaluation as food contact materials, Food Chem. Toxicol. 142 (2020), 111457, https://doi.org/10.1016/j.fct.2020.111457.

[48] W.S. Oliveira, J.O. Monsalve, C. Nerín, M. Padula, H.T. Godoy, Characterization of odorants from baby bottles by headspace solid phase microextraction coupled to gas chromatography-olfactometry-mass spectrometry, Talanta 207 (2020), 120301, https://doi.org/10.1016/j.talanta.2019.120301.

[49] L. Žniderščič, A. Mlakar, H. Prosen, Development of a SPME-GC-MS/MS method for the determination of some contaminants from food contact materials in beverages, Food Chem. Toxicol. 134 (2019), 110829, https://doi.org/10.1016/j.fct.2019.110829.
[50] M.C. Ortiz, S. Sanllorente, A. Herrero, C. Reguera, L. Rubio, M.L. Oca, L. Valverde-Som, M.M. Arce, M.S. Sánchez, L.A. Sarabia, Three-way PARAFAC decomposition of chromatographic data for the unequivocal identification and quantification of compounds in a regulatory framework, Chemometr. Intell. Lab. Syst. 200 (2020), 104003, https://doi.org/10.1016/j.chemolab.2020.104003.
[51] L. Rubio, M.C. Ortiz, L.A. Sarabia, Identification and quantification of carbamate pesticides in dried lime tree flowers by means of extraction-emission molecular fluorescence and parallel factor analysis when quenching effect exists, Anal. Chim. Acta 820 (2014) 9–22, https://doi.org/10.1016/j.aca.2014.02.008.
[52] R. Bro, H.A.L. Kiers, A new efficient method for determining the number of components in PARAFAC models, J. Chemom. 17 (2003) 274–286, https://doi.org/10.1002/cem.801.
[53] S. Bratinova, B. Raffael, C. Simoneau, Guidelines for Performance Criteria and Validation Procedures of Analytical Methods Used in Controls of Food Contact Materials, Luxembourg, first ed., 2009. EUR 24105 EN), https://publications.jrc.ec.europa.eu/repository/handle/JRC53034. (Accessed May 2022). accessed.
[54] G.E.P. Box, N.R. Draper, Response Surfaces, Mixtures and Ridge Analyses, John Wiley, 2007.
[55] A. Inselberg, Parallel Coordinates: Visual Multidimensional Geometry and its Applications, Springer, Dordrecht, Heidelbeg, 2009.
[56] P.J. Rousseeuw, K. Van Driessen, An algorithm for positive-breakdown methods based on concentration steps, in: W. Gaul, O. Opitz, M. Schader (Eds.), Data Analysis: Scientific Modeling and Practical Application, Springer-Verlag, New York, 2000, pp. 335–346.
[57] ISO 11843, Capability of Detection, Part 1: Terms and Definitions and Part 2: Methodology in the Linear Calibration Case, International Organization for Standardization, 2000.
[58] M.C. Ortiz, L.A. Sarabia, I. García, D. Giménez, E. Meléndez, Capability of detection and three-way data, Anal. Chim. Acta 559 (2006) 124–136, https://doi.org/10.1016/j.aca.2005.11.069.
[59] R. Maranna, Robust statistical methods, in: M. Lovric (Ed.), International Encyclopedia of Statistical Science, Springer, Berlín, Heidelberg, 2011, pp. 1244–1248, https://doi.org/10.1007/978-3-642-04898-2_496.
[60] C. Bach, X. Dauchy, I. Severin, J.F. Munoz, S. Etienne, M.C. Chagnon, Effect of temperature on the release of intentionally and non-intentionally added substances from polyethylene terephthalate (PET) bottles into water: chemical analysis and potential toxicity, Food Chem. 139 (2013) 672–680, https://doi.org/10.1016/j.foodchem.2013.01.046.